

Change of interference pattern using fundamental and second-harmonic wavelengths by phase shift of a beam

Yoshiki Nakata · Yoshiki Matsuba ·
Keiichi Murakawa · Noriaki Miyanaga

Received: 3 November 2013 / Accepted: 4 March 2014 / Published online: 26 March 2014
© Springer-Verlag Berlin Heidelberg 2014

Abstract Interference pattern of two different wavelengths, forming a four-sided pyramid consisting of eight beams, is discussed. Synchronization between two wavelengths having a multiple relationship, which corresponds to mixing of fundamental and second-harmonic generation wavelengths, forms a stationary interference pattern successfully. Phase shift variation of a beam changes the basic pattern of interference. This technique can be a new scheme for multi-wavelength material processing with periodic structure and will increase the variation of meta-atoms fabricated by interfering femtosecond laser processing.

1 Introduction

Formation of interference is an intrinsic nature of laser. Our group has been investigating direct material processing using interference patterns of ultra-short pulse beams. We fabricated 2D and 3D periodic structures by a single process [1, 2], for example, nanowhiskers with summit curvature radii of 4 nm were successfully fabricated by a solid–liquid–solid (SLS) process using a gold thin film [2]. In addition, the period can be shortened to less than 1 μm using second-harmonic generation (SHG) of a femtosecond laser [3]. We extended this methodology by controlling the phase and amplitude shift between interfering beams and reported the designing of interference pattern such as metal-hole-array (MHA), split-ring-resonator (SRR), cross, etc. [4–8], of which some are useful for the fabrication of metamaterials. To increase the design of meta-atom and

extend the applicability of this scheme, wavelength mixing can be an additional parameter. In addition, material processing at two different wavelengths is a well-known technique applied to precise and efficient material processing [9]. If interference pattern could be formed by mixing different wavelengths, it could be another method for periodic processing of wide bandgap materials. On the other hand, it has not been investigated in detail.

In this study, we numerically simulated the interference pattern of two wavelengths with multiple relationships, such as fundamental and SHG beam. Each wavelength consists of four beams, and they correlate on the surface of a target. The pattern variation as a function of the phase shift of a beam of fundamental or SHG is surveyed.

2 Simulation model of interference pattern

In this simulation, we used eight counter-propagating coherent beams forming a quadrangular pyramid, as shown in Fig. 1. Each group of four beams is drawn in orange for the fundamental wavelength or purple for the SHG wavelength, and these correlate on the surface of a target where $z = 0$. The angle between the beams and the target normal (polar angle) is set to $\theta_{\text{int}} = 14.6^\circ$ and $\lambda_{\text{fund.}} = 2\lambda_{\text{SHG}} = 785 \text{ nm}$, in accordance with the results previously reported where we used a fundamental beam [2]. The azimuthal angles are set to $\phi_m = 0, \pi/2, 2\pi/2, 3\pi/2$ for both wavelengths, thereby configuring a four-sided pyramid. An interference pattern of coherent plane waves is calculated by the following equation on the basis of the principle of superposition of electric fields:

$$I(x, y, z) = \int \left| \sum_{n=1,2,\dots}^N E_n(E_{n0}, x, y, z, k_n, \theta_{\text{int}}, \phi_n, \omega_n, \alpha_n, t) \right|^2 dt, \quad (1)$$

Y. Nakata (✉) · Y. Matsuba · K. Murakawa · N. Miyanaga
Institute of Laser Engineering, Osaka University,
2-6 Yamadaoka, Suita 565-0871, Japan
e-mail: nakata-y@ile.osaka-u.ac.jp

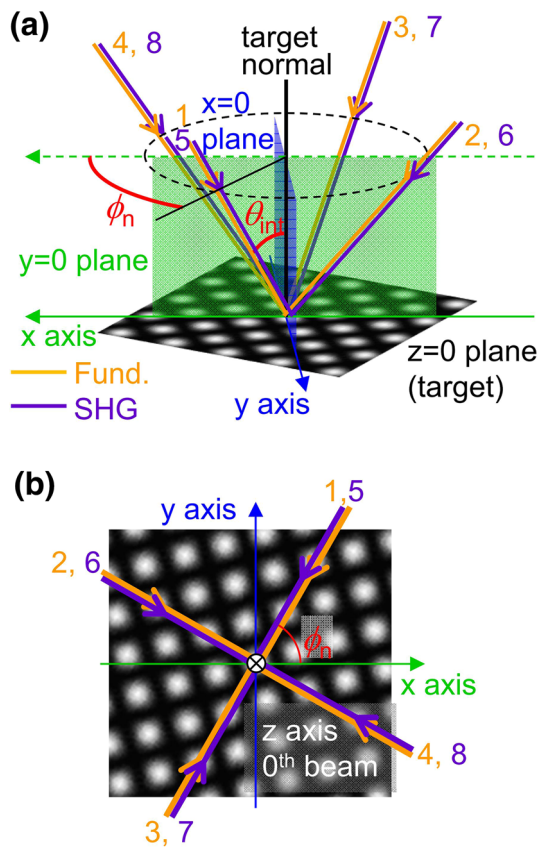


Fig. 1 Schematic of four fundamental and four SHG interfering beams forming a quadrangular pyramid. Orange and purple rays correspond to fundamental and SHG beams, respectively. **a** A bird's eye view and **b** a top-down view of (a)

where E_n represents the electric field intensity of the beams illustrated in Fig. 1. The electric fields of each beam can be expressed as follows:

$$E_n(E_{n0}, x, y, z, k_n, \theta_{int,n}, \phi_n, \alpha_n, t) = E_{n0} \cos(k_n \cos \theta_{int,n} * z + k_n \sin \theta_{int,n} * (-x \cos \phi_n - y \sin \phi_n) - ck_n t + \alpha_n), \tag{2}$$

where ω_n is the angular frequency; E_{n0} is the amplitude of the electric field, which is linear to the square root of the beam intensity I_{n0} , and α_n is the phase shift between beams. The suffixes “1”, “2”, “3”, and “4” denote the fundamental wavelength, and suffixes “5”, “6”, “7”, and “8” denote the SHG wavelength. In addition, $2\omega_{fund} = \omega_{SHG}$, and the electric field intensity E_{n0} is set to 1, or 0 arb. unit at both wavelengths. Equation (1) is integrated for $t = \lambda_{fund.}/c = 2\lambda_{SHG.}/c$, which corresponds to a single cycle for the fundamental wavelength and to a double cycle for the SHG wavelength. Parameters of electric field intensity and phase shift are summarized in Table 1.

Table 1 Parameters of the interfering two wavelength beams

	E1– E4	E5– E8	α_1/π	$\alpha_2/\pi - \alpha_4/\pi$	α_5/π	$\alpha_6/\pi - \alpha_8/\pi$	$r = \frac{F_{peak}}{F_{av.}}$
Figure 2a	1	0	0	0	0	0	4.00
Figure 2b	0	1	0	0	0	0	4.00
Figures 3a, 4a	1	1	0	0	0	0	4.00
Figure 3b	1	1	0.25	0	0	0	3.78
Figure 3c	1	1	0.50	0	0	0	3.28
Figure 3d	1	1	0.75	0	0	0	2.72
Figure 3e	1	1	1.00	0	0	0	2.50
Figure 4b	1	1	0	0	0.50	0	3.55
Figure 4c	1	1	0	0	0.75	0	3.13
Figure 4d	1	1	0	0	1.00	0	2.60

3 Results and discussions

Interference patterns of two fundamental and SHG wavelength are shown in Fig. 2a and b, respectively. The sets of six diagrams beside each interference pattern are contour plots at different thresholds of the corresponding interference patterns, as explained in the rightmost inset. The fluence in the orange (brighter) region is over 5% (0.50) of the peak fluence in the case of (i). The threshold T is then changed as follows: (ii) 10% (0.10), (iii) 15% (0.15), (iv) 20% (0.20), (v) 50% (0.50), and (vi) 80% (0.80). The area is $4 \mu\text{m}^2 \times 4 \mu\text{m}^2$ for every contour plot. Here, the contour lines can be correlated to the processed regions in interfering laser processing. In addition, the ratio r of peak fluence F_{peak} to the averaged fluence $F_{av.}$ is also shown in Table 1. Here, the fluence on the borderline in a contour plot is $F_{peak} \times T$. If this value is same with the processing threshold of a material F_T , the surface is ablated according to the corresponding contour plot. In this case, the averaged fluence that should be used is explained as follows:

$$F_{av.} = \frac{F_T}{rT}. \tag{3}$$

It seems that peaks of interference patterns are in matrix with the period according to the equation $\lambda/\sqrt{2} \sin \theta$. The shapes of orange and blue region, corresponding to processed or not-processed area, change as the fluence. The shape is small circle in case of lower fluence as shown in Fig. 2a(vi) and b(vi). On the other hand, it is round square in the case of higher fluence as shown in Fig. 2a(i) and b(i).

The interference patterns of fundamental and SHG beams as a function of the phase shift of a fundamental beam are summarized in Fig. 3. It seems that interference pattern of two different wavelengths is formed successfully without sweep. The period between the larger peaks at

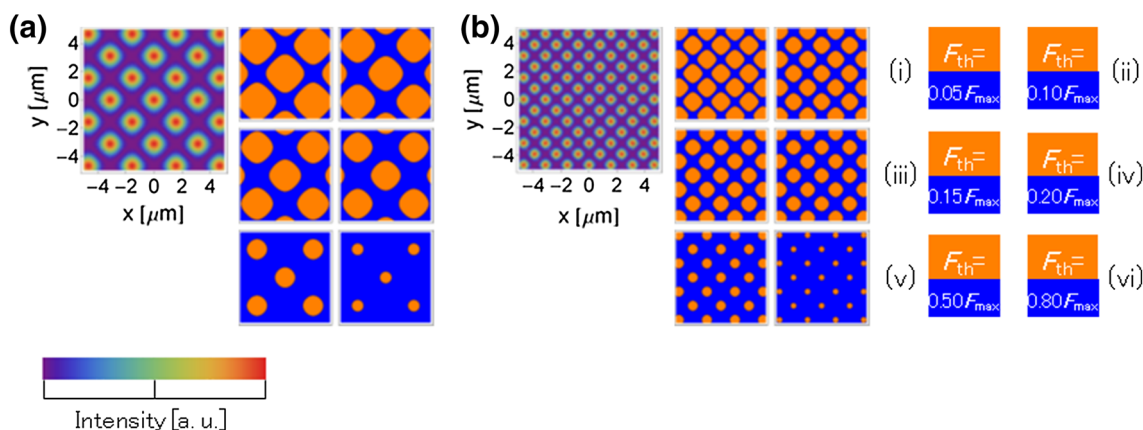


Fig. 2 Interference patterns of **a** fundamental and **b** SHG without wavelength mixing and phase shift. The sets of six diagrams beside each interference pattern are contour plots at different thresholds of

the corresponding interference patterns, as explained in the *rightmost inset*. The fluence in the *orange* (brighter) region is (i) over 5 % of the peak fluence, (ii) 10 %, (iii) 15 %, (iv) 20 %, (v) 50 %, and (vi) 80 %

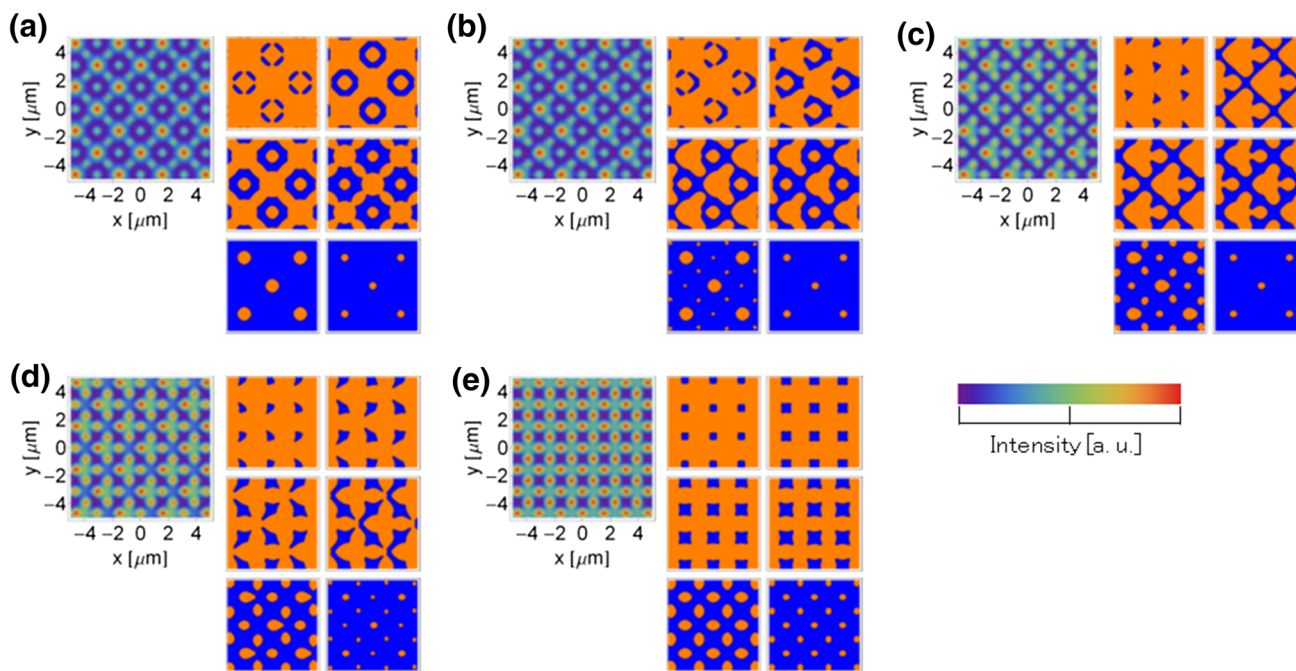


Fig. 3 Interference patterns as a function of the phase shift of a fundamental beam. **a** $\phi_1 = 0$, **b** $\phi_1 = \pi/4$, **c** $\phi_1 = 2\pi/4$, **d** $\phi_1 = 3\pi/4$, **e** $\phi_1 = 4\pi/4$. The electric field intensities are $E_{fund.} =$

$E_{SHG} = 1$ (arb. u.), respectively. The *color scale* intensity is normalized to each peak brightness

higher fluence is the same with that at fundamental wavelength as shown in Fig. 2a. It seems that residual weak peaks appear between the larger peaks. In the contour plots in Fig. 3, it is shown that the shape of blue region changes with fluence as in the case of Fig. 2. The shape corresponds to that of the meta-atom, where a metal thin film is ablated by the pattern and the blue and lower fluence region remains. The shape is four cut SRR in the case of Fig. 3a(i), which will be useful for permeability control at shorter wavelength [7]. With the phase shift of $\alpha_1 = \pi/4$,

the shape is single SRR as shown in Fig. 3b(ii). Finally, the shape is square with the phase shift of $\alpha_1 = \pi$, as shown in Fig. 3e(i), (ii), and (iii).

The interference patterns of fundamental and SHG beams as a function of the phase shift of a SHG beam is summarized in Fig. 4. Single SRR appears with $\alpha_5 = \pi/2$ as shown in Fig. 4b(ii), but the direction of cut is opposite compared to Fig. 3b(ii) case. With the phase shift of $\alpha_5 = \pi$, ellipsoidal MHA can be obtained as shown in Fig. 4d(vi).

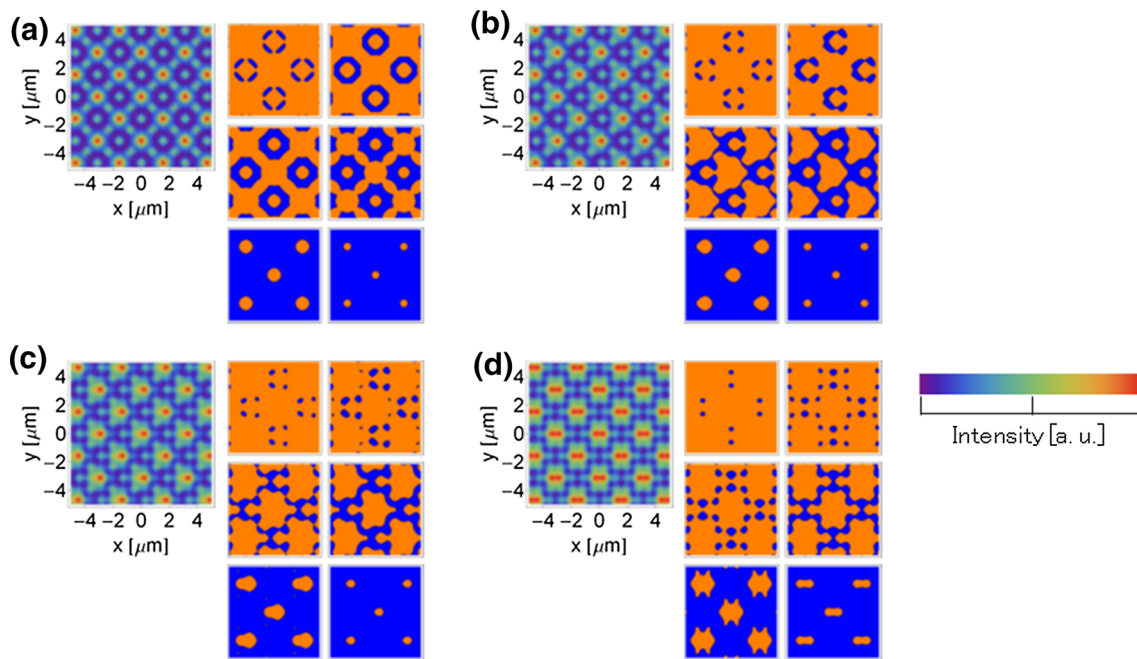


Fig. 4 Interference patterns as a function of the phase shift of a SHG beam. **a** $\phi_5 = 0$, **b** $\phi_5 = 2\pi/4$, **c** $\phi_5 = 3\pi/4$, **d** $\phi_5 = 4\pi/4$. The electric field intensities are $E_{\text{fund.}} = E_{\text{SHG}} = 1$ (arb. u.), respectively. The *color scale* intensity is normalized to each peak brightness

4 Conclusion

Various interference patterns can be obtained using two different wavelengths with multiple relation. The pattern changes as a function of the phase shift of a fundamental or SHG beam. The unit figures of lower fluence regions include meta-atoms such as MHA, round square MHA, four SRR, single SRR, and ellipsoidal MHA. They appear in square lattice, so they are very useful for the fabrication of corresponding metamaterials. In addition, a collinear irradiation system of two nanosecond excimer lasers is useful for high-quality and high-efficiency material processing via a multi-wavelength excitation process [9]. So, our scheme which uses two different wavelengths can be a new technique for periodic processing of wide bandgap material. From a practical point of view, a beam that consists of two wavelengths with multiple relationship can be simply generated by a nonlinear crystal. In our technique, they can be correlated by adaptive or diffractive optics with focusing system [1–6, 10]. This scheme will widen the capability of laser processing with multi-wavelength beams.

Acknowledgments This research was financially supported by the Japan Society for the Promotion of Science (JSPS) through a Grant-in-Aid for Scientific Research (B) (No. 23360035).

References

1. Y. Nakata, T. Okada, M. Maeda, *Jpn. J. Appl. Phys.* **42**, L1452 (2003)
2. Y. Nakata, N. Miyanaga, K. Momoo, T. Hiromoto, *Appl. Surf. Sci.* **274**, 27 (2013)
3. Y. Nakata, K. Murakawa, N. Miyanaga, and K. Momoo, *Appl. Phys. Express* **5** 102703 (2012). SHG
4. Y. Nakata, T. Hiromoto, N. Miyanaga, *Appl. Phys. A* **101**, 471 (2010)
5. Y. Nakata, K. Murakawa, K. Sonoda, K. Momoo, N. Miyanaga, T. Hiromoto, *Appl. Phys. A* **112**, 191 (2013)
6. Y. Nakata, K. Murakawa, K. Sonoda, K. Momoo, *Appl. Opt.* **51**, 5004 (2012)
7. A. Ishikawa, T. Tanaka, S. Kawata, *J. Opt. Soc. Am. B* **24**, 510 (2007)
8. C.M. Soukoulis, M. Wegener, *Nat. Photon.* **5**, 523 (2011)
9. K. Obata, K. Sugioka, T. Akane, N. Aoki, K. Toyoda, K. Midorikawa, *Appl. Phys. A* **73**, 755 (2001)
10. Y. Hayasaki, T. Sugimoto, A. Takita, N. Nishida, *Appl. Phys. Lett.* **87**, 031101 (2005)